Dissolved sulfide distributions in the water column and sediment pore waters of the Santa Barbara Basin

JAMES S. KUWABARA,[1,]* ALEXANDER VAN GEEN,[2] DANIEL C. MCCORKLE,[3] and JOAN M. BERNHARD[4]

[1]U.S. Geological Survey, Water Resources Division, Menlo Park, California 94025, USA
[2]Lamont-Doherty Earth Observatory, Columbia University, Palisades, New York 10964, USA
[3]Woods Hole Oceanographic Institute, Woods Hole, Massachusetts 02543, USA
[4]University of South Carolina, Columbia, South Carolina 29208, USA

Abstract—Dissolved sulfide concentrations in the water column and in sediment pore waters were measured by square-wave voltammetry (nanomolar detection limit) during three cruises to the Santa Barbara Basin in February 1995, November–December 1995, and April 1997. In the water column, sulfide concentrations measured outside the basin averaged 3 ± 1 nM ($n = 28$) in the 0 to 600 m depth range. Inside the basin, dissolved sulfides increased to reach values of up to 15 nM at depths >400 m. A suite of box cores and multicores collected at four sites along the northeastern flank of the basin showed considerable range in surficial (<0.5 cm) pore-water sulfide concentrations: <0.008, 0.01, 0.02, to as much as 0.4 μM at the 340, 430, 550, and 590 m sites, respectively. At a core depth of 10 cm, however, pore–water sulfides exhibited an even wider range: 0.005, 0.05, 0.1, and 100 μM at the same sites, respectively. The sulfide flux into the deep basin, estimated from water-column profiles during three cruises, suggests a fairly consistent input of 100–300 nmole m^{-2} h^{-1}. In contrast, sulfide fluxes estimated from pore-water sulfide gradients at the sediment water interface were much more variable (-4 to 13,000 nmole m^{-2} h^{-1}). Dissolved silicate profiles show clear indications of irrigation at shallow sites (340 and 430 m) in comparison to deeper basin sites (550 and 590 m) with low (<10 μM) bottom-water dissolved-oxygen concentrations. Pore-water profiles indicate ammonia generation at all sites, but particularly at the deep-basin 590 m site with concentrations increasing with sediment depth to >400 μM at 10 cm. Decreases in water-column nitrate below the sill depth indicate nitrate consumption (-55 to -137 μmole m^{-2} h^{-1}) similar to nearby Santa Monica Basin. Peaks in pore-water iron concentrations were generally observed between 2 and 5 cm depth with shallowest peaks at the 590 m site. These observations, including observations of the benthic microfauna, suggest that the extent to which the sulfide flux, sustained by elevated pore-water concentrations, reaches the water column may be modulated by the abundance of sulfide-oxidizing bacteria in addition to iron redox and precipitation reactions. *Copyright © 1999 Elsevier Science Ltd*

1. INTRODUCTION

One reason for continued interest in low-oxygen environments is that high-resolution paleoclimatic information can be extracted from sediments which are not bioturbated by macrofauna (Soutar, 1971; Shimmield and Price, 1986; Petersen et al., 1991; Behl and Kennett, 1996). The motivation for the present study of dissolved sulfides in the Santa Barbara Basin, one of the Southern California borderland basins, is that certain metals such as Cd and Mo precipitate in reducing sediment, most likely due to the formation of insoluble sulfide phases (Jacobs et al., 1985; Emerson and Huested, 1991; Rosenthal et al., 1995; Helz et al., 1996; Piper and Isaacs, 1996). Cadmium and molybdenum enrichments observed in marine sediment deposits have been used to infer more reducing conditions in the past caused by either decreased ocean ventilation, increased productivity, or both (Rosenthal et al., 1995; van Geen et al., 1995; Crusius, 1996; Zheng et al., in preparation). However, the conditions under which the so-called authigenic precipitation of Cd and Mo take place are not well known. The Santa Barbara Basin is particularly well-suited to study interactions

between dissolved sulfides and redox-sensitive paleoceanographic proxies because the sea floor of this basin traverses a wide range of bottom-water oxygen concentrations within a geographically restricted region where the nature and quantity of sediment deposited is fairly uniform (Zheng et al., in prepatation).

Redox conditions in the water column of the Santa Barbara Basin today are intermediate between conditions in permanently anoxic systems such the Black Sea and oxygenated open-ocean water. Circulation and productivity are the primary processes that determine these low-oxygen conditions. Dissolved sulfide concentrations reported for these environments range from >400 μM in the Black Sea (e.g., Karl, 1978; Luther et al., 1991; Millero, 1991) to <0.01 μM in the oxic water column of the eastern Mediterranean Sea and northwest Atlantic Ocean (Luther and Tsamakis, 1989). In seasonally anoxic marine systems such as Saanich Inlet, water-column hydrogen sulfide (H_2S) concentrations range from <1 to ~ 20 μM (Richards, 1965; Emerson and Huested, 1991). To our knowledge, dissolved sulfide concentrations below the ~ 1 μM detection limit for the standard colorimetric method of Cline (1969) have never been reported in the Santa Barbara Basin. At the same time, micromolar sulfide concentrations, measured in pore waters in the basin sediments, at a distance of <10 cm below the

*Address reprint requests to Dr. J. S. Kuwabara, U.S. Geological Survey, Water Resources Division, Menlo Park 94025, CA, USA; E-mail: kuwabara@usgs.gov.
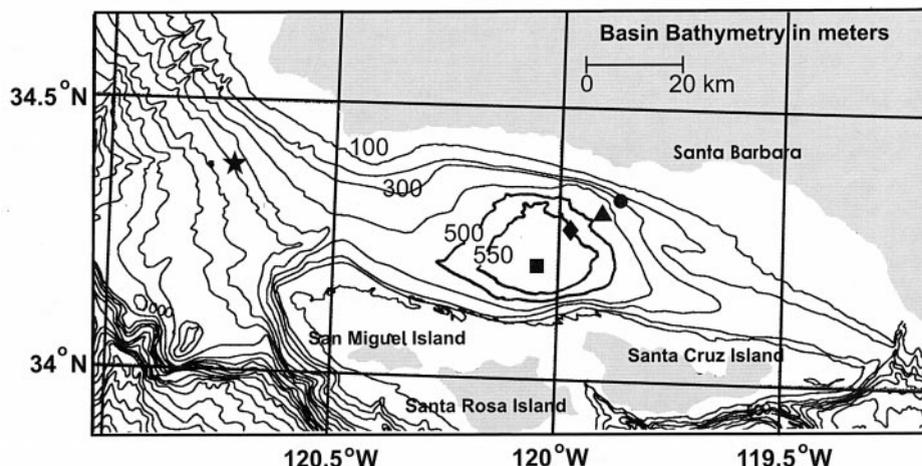
Fig. 1. Bathymetric map of the coring and hydrocast stations within the basin at 590 m (square), 550 m (diamond), 430 m (triangle), and 340 m (circle), and outside the basin (590 m, star). Symbols on this map are used in later figures to indicate data from corresponding sampling locations.

sediment–water interface (Reimers et al., 1990), suggest a flux into the water column.

In this study, we used a voltammetric technique (Kuwabara and Luther, 1993) to measure total dissolved (0.2 μm filtered) sulfides in pore waters and in the water column aboard ship during three separate cruises. Dissolved-oxygen and nitrate profiles in the water column inside and outside of the basin, as well as pore-water silicate, ammonia, and iron profiles are also presented to facilitate the intepretation of the sulfide data, and to provide supporting evidence for the magnitude of temporal and spatial redox variability in the basin.

2. EXPERIMENTAL METHODS

Water-column samples were collected at two deep-basin sites (550 and 590 m; Fig. 1) with lever-action 2.5 l Niskin bottles attached to a wire and triggered by messengers during a February 1995 cruise to the Santa Barbara Basin on board the R. V. Robert Gordon Sproul. Dissolved-oxygen (DO) concentrations were measured by Scripps Oceanographic Data Facility without replication at the end of the first cruise

by Winkler titration. Bottom-water (~2 m above the bottom) DO concentrations at the coring sites were measured on board in duplicate by the micro-Winkler method (Broenkow and Cline, 1969). During the two subsequent cruises in November–December 1995 and April 1997 on board the R. V. Pt. Sur, water-column samples were collected with 10 l Niskin bottles mounted on a 12-position rosette. Water-column DO concentrations were determined at 1 m intervals with an oxygen probe mounted on the rosette system, in addition to micro-Winkler measurements for bottom water. Seawater density was calculated from pressure, temperature, and salinity measurements taken from additional probes on the rosette (Fofonoff and Millard, 1983).

Sediment cores described in this paper are indexed by type of coring (B for Soutar box corer, and M for multicorer), site depth (m), and cruise sequence (1 for February 1995, 2 for November 1995, and 3 for April 1997; see Table 1). During the February cruise, sediment was collected at two depths with a Soutar box corer (B590-1 and B550-1). During November–December 1995 (M580-2, M430-2, M340-2) and April 1997 (M590-3, M550-3, M430-3) cruises, sediment was collected with a multicorer that provided a set of eight subcores per deployment.

Subcores from the box core and individual multicores were extruded under nitrogen in a glove bag within a refrigerated van to limit sample oxidation. Near the sediment–water interface, cores were typically

Table 1. Water-column and pore-water sampling in the vicinity of the Santa Barbara Basin. Core designations are given in the following format: type of coring (B for Soutar box corer, and M for multicorer), site depth (m), and cruise sequence (1 for February 1995, 2 for November 1995, and 3 for April 1997. In contrast to other water-column sampling, two hydrocasts were taken at the 590 m site on 29 and 30 November 1995; the first sampling the water column at depths ≤440 m and the second sampling at depths ≥440 m.

| Date	Core designation	Latitude North	Longitude West	Depth (m)	Operation
2/16/95	—	34°15.63′	120°0.33′	590	Hydrocast
2/16/95	B590-1	34°13.14′	120°1.92′	590	Soutar Box Core
2/17/95	B550-1	34°16.93′	119°58.54′	560	Soutar Box Core
11/29/95	—	34°13.75′	120°2.79′	590	Hydrocast
11/30/95	M430-2	34°18.57′	119°54.18′	430	Multicore-A
11/30/95	—	34°13.52′	120°1.56′	590	Hydrocast
12/1/95	M580-2	34°13.85′	120°2.89′	580	Multicore-C
12/2/95	M340-2	34°20.06′	119°52.25′	340	Multicore-E
12/2/95	—	34°22.16′	120°43.37′	590	Hydrocast
4/25/97	M590-3	34°13.82′	120°2.94′	590	Multicore-G
4/26/97	—	34°13.91′	120°3.35′	590	Hydrocast
4/26/97	M430-3	34°18.64′	119°54.22′	440	Multicore-H
4/26/97	—	34°22.14′	120°43.44′	590	Hydrocast
4/27/97	M550-3	34°16.07′	119°58.04′	550	Multicore-I
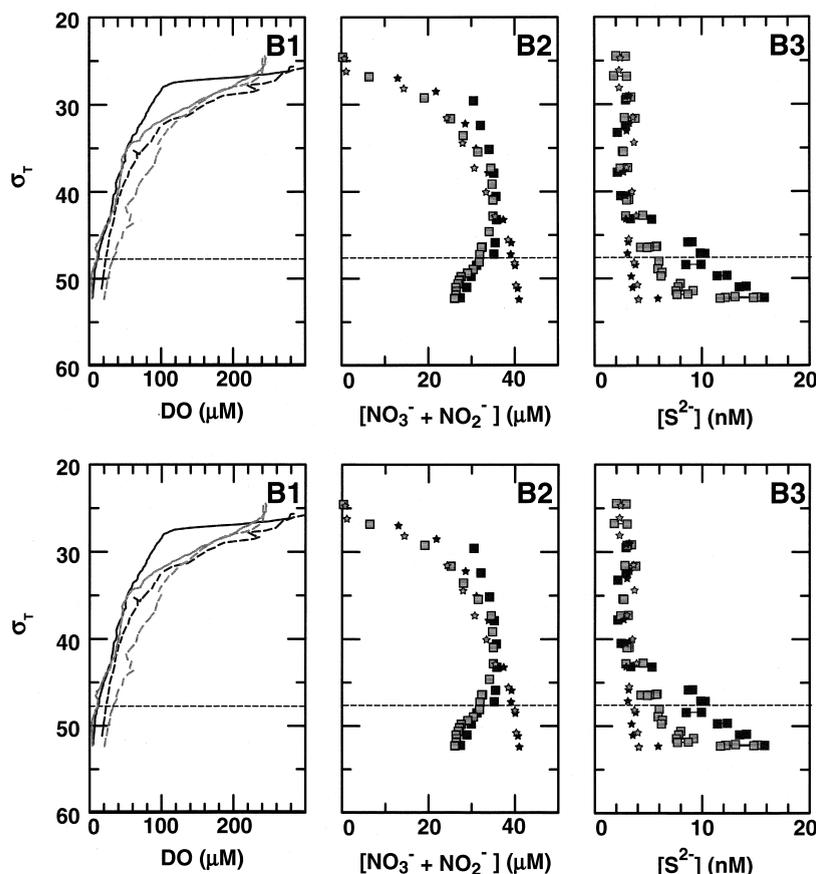
Fig. 2. A comparison of water-column redox conditions at hydrocast stations within and outside the basin relative to depth (panel A) and density (panel B) for: (1) dissolved oxygen (DO), (2) nitrate and nitrite, and (3) sulfides (note nanomolar units). Open, shaded, and dark symbols denote data from February 1995, December 1995, and April 1997 cruises, respectively. Squares and stars denote concentrations at the deep basin site and outside the basin, respectively. For DO measurements by oxygen probe, solid and hatched lines represent data from sites within and outside the basin, respectively. Discrete DO concentrations are also shown of the bottom water by micro-Winkler analyses, and of the water column in February 1995 by standard Winkler titration. The horizontal hatched lines at 480 m (panel A) and σ_T (density in kg m^{-3}—1000) of 48 (panel B) indicate the approximate sill depth and σ_T at sill depth. Due to the absence of CTD data for the February 1995 hydrocast, data from that cast are plotted only in panel A.

sectioned with a minimum interval of 0.352 cm (i.e., a mid-point of 0.176 cm), and the resulting wet sediment was packed into scintillation vials (20 ml) before centrifugation at 5,000 rpm for 5 min. Further downcore, coarser sectioning was used (≥ 0.5 cm) that required 50 ml polypropylene tubes for centrifugation. The supernatant was filtered under nitrogen through 0.45 μm Gelman Acrodisc syringe filters. Results from the analyses of these filtered samples will hereafter be referred to as "dissolved" concentrations. The fraction of pore-water sample used to measure silicate, ammonia, and iron was acidified with 12 N HCl (5 μl per ml). Unacidified pore-water samples (~ 5 ml) were stored in a closed syringe and analyzed for dissolved sulfide within a few hours by both square-wave voltammetry (Kuwabara and Luther, 1993) and a modification of the colorimetric method of Cline (1969). The voltammetric method that was used, due to the concentration range of interest in this suboxic environment (nM to mM) and the decision not to store samples, did not discriminate between dissolved hydrogen–sulfide and polysulfide species. Methods to determine sulfur speciation in marine pore waters ($> 10^1$ μM; Luther et al., 1985) require manipulation and processing of subsamples (e.g., reaction with sodium sulfite, purging, acidification, and heating).

Dissolved nitrate + nitrite concentrations (hereafter referred to as nitrate) for all water-column samples were measured at Lamont-Doherty in acidified samples (60 μl of 12 N Ultrex HCl per 60 ml) by colorimetry (Strickland and Parsons, 1968; Johnson and Petty, 1983)

adapted to flow injection analysis with a Lachat QuikChem 8000 analyzer. Results from the February 1995 cruise agreed ($\pm 5\%$) with nitrate measurements made by Scripps Oceanographic Data Facility on samples preserved by freezing. Pore-water silicate concentrations were also measured by colorimetry with the Lachat instrument, following dilution with de-ionized water obtained from a Millipore MQ system (> 18 MΩ). Pore-water iron concentrations were measured by graphite-furnace atomic absorption spectroscopy on a Hitachi Zeeman-8200 instrument. Samples were diluted with 1% Seastar HNO$_3$, and concentrations were determined by the method of standard additions. Precision of the dissolved Fe and nutrient measurements was $\pm 5\%$.

Trade names are provided for identification purposes only and do not constitute endorsement by the U.S. Geological Survey.

3. RESULTS

3.1. Water Column

The observed decrease in DO concentrations with depth outside the basin, from > 200 μM in surface waters to 16 and 21 μM in December 1995 and April 1997 at 600 m depth, reflects the pronounced oxygen minimum zone centered at ~ 800 m depth (Fig. 2A1) that is characteristic of the northeast

Pacific (Kester, 1975). The oxygen content of the water column in the Santa Barbara Basin below the depth of the western sill at ~480 m was further reduced to as low as 1.3 μM relative to external source waters by the combined effects of local oxygen consumption and restricted circulation. The decrease in water-column nitrate concentration to as low as 15 μM in February 1995 (Fig. 2A2), and to 26 μM in November 1995 inside the basin, relative to 40 μM on the same density surface outside the basin (Fig. 2B2), is another indication of additional oxidant consumption within the basin due to organic matter decomposition. The density of deep water within the basin (σ_T of 52.2 at 580 m) closely corresponds to a depth of approximately 575 m outside the basin.

Dissolved sulfide concentrations measured in the water column outside the basin average 3 ± 1 nM in the 0–600 m depth range. In the upper part of the water column above the basin, sulfide concentrations were very similar (Fig. 2A3). Below ~400 m depth, however, an increase in dissolved sulfide concentrations was consistently observed with depth and density inside the basin up to 15 nM (Figs. 2A3 and 2B3).

3.2. Sediment Characteristics

In February 1995, deep-basin cores had a brown surface layer of ~1 cm thickness; similar to annual sedimentation in the basin (0.4–0.7 cm yr^{-1}, Reimers et al., 1990). In the following December (M580-2), a thin orange veneer overlaid that brown layer. The deep-basin cores in April 1997 (M590-3 and M550-3) exhibited tufts of the sulfide-oxidizing bacterium *Beggiatoa*, which had not been seen during the February and December 1995 cruises. These structures have been hypothesized to reflect an attempt by the colony to move into the more oxidizing environment just above the sediment–water interface (Møller et al., 1985).

Laminated sediments were observed below the oxidized surface layer in the deep-basin cores (590 and 550 m). Formation of these laminations is due to seasonal changes in biogenic and lithogenic sources (Sholkovitz and Gieskes, 1971; Reimers et al., 1990; Thunell et al., 1995). By contrast, cores from shallower sites at 430 and 340 m exhibited thick (>2 cm), brown, surface-oxidized layers, and no evidence of laminae deeper in the cores. Large burrowing polychaetes and foraminiferal species associated with higher bottom-water oxygen concentrations were observed at the 430 and 340 m sites (DO > 15 μM), but not at the deep basin sites (DO < 5 μM; Bernhard et al., 1997). Where relatively high bottom-water DO concentrations permit the presence of abundant macrofauna, their burrowing and irrigation presumably contribute to the less reduced (or more oxic) pore-water chemistry observed at these shallower sites.

In M590-3, ^{210}Pb and ^{234}Th profiles show that about 12 cm of sediment was removed a few months to weeks before our cruise in April 1997 (Zheng et al., in preparation, 1998). Since the multicorer did not over penetrate, and the surficial microbial population was reestablished, we can only speculate that perhaps previous sampling efforts disturbed the sediment surface at this site. Therefore, this core is not discussed further.

3.3. Pore Waters

Dissolved-sulfide concentrations measured in pore waters of Santa Barbara Basin varied over several orders of magnitude. At the shallowest sample site, concentrations in the upper 10 cm of the sediment were only slightly greater than water-column concentrations (Fig. 3A1). However, in M430-2 and M430-3, dissolved-sulfide concentrations increased from near-water column levels at the surface to 0.05 μM within the top 10 cm. Surficial-sulfide levels were not markedly higher in M550-1 and M550-3, although concentrations were ≥0.3 μM within the upper 10 cm in February 1995 (Fig. 3A3). Only at the deepest site (590 m) did pore-water sulfides increase to levels >1 μM in the upper 10 cm of the sediment. A comparison between dissolved-sulfide analytical procedures for the three cruises (Fig. 3A4) showed good agreement ($r^2 = 0.93$, $n = 47$) for samples with concentrations above the detection limit for the colorimetric method (~1–>100 μM).

Pore-water silicate concentrations increased less rapidly in shallow cores from the basin slope (M430-2, M340-2, and M430-3) than those from the deep basin (Fig. 3B). In addition, these shallow cores showed subsurface silicate depletions not observed in the deep-basin cores. At a core depth of 10 cm, the silicate concentrations ranged between 420 μM for M340-2 and 680 μM for M580-2.

Pore-water ammonia profiles were very similar at the 340, 430, and 550 m sites with concentrations increasing to <200 μM with depth (Fig. 3C). Dramatically different ammonia profiles were observed in B590-1 and M580-2 as indicated by steeper concentration gradients near the sediment–water interface (<5 cm; Table 2), and pore-water concentrations >400 μM at a core depth of 10 cm (Fig. 3C4).

Dissolved Fe concentrations in pore waters at all sites ranged from <1 to 150 μM (Fig. 3D). Highest concentrations commonly occurred between 2 and 5 cm depth. At the 340 and 430 m sites, Fe concentrations at 10 cm depth were approximately 50 μM. This contrasts with the deepest site where Fe concentrations decreased to <5 μM within the upper 5 cm of the sediment.

4. DISCUSSION

An integrated examination of water-column and pore-water profiles for redox-sensitive solutes provides boundary conditions from which interfacial processes that regulate the transport and distribution of these solutes can be identified. The transect of coring sites used in our four cruises between February 1995 and April 1997, represents an opportunity to quantify spatial and temporal variability of such processes within ecosystems like the Santa Barbara Basin.

4.1. Spatial Variability of Sulfide and Nutrient Fluxes

An estimate of the dissolved-sulfide flux out of the sediments (F) can be made with the water-column data (Fig. 2A3) from within the basin using the following equation:

$F = K_z (dC/dz)$, where K_z is the vertical eddy diffusivity and dC/dz is the vertical concentration gradient in the basin computed by exponential fit (Klump and Martens, 1981), evaluated at the sediment–water interface, using data from the sediment–water interface to the sill depth (590–480 m). Chung
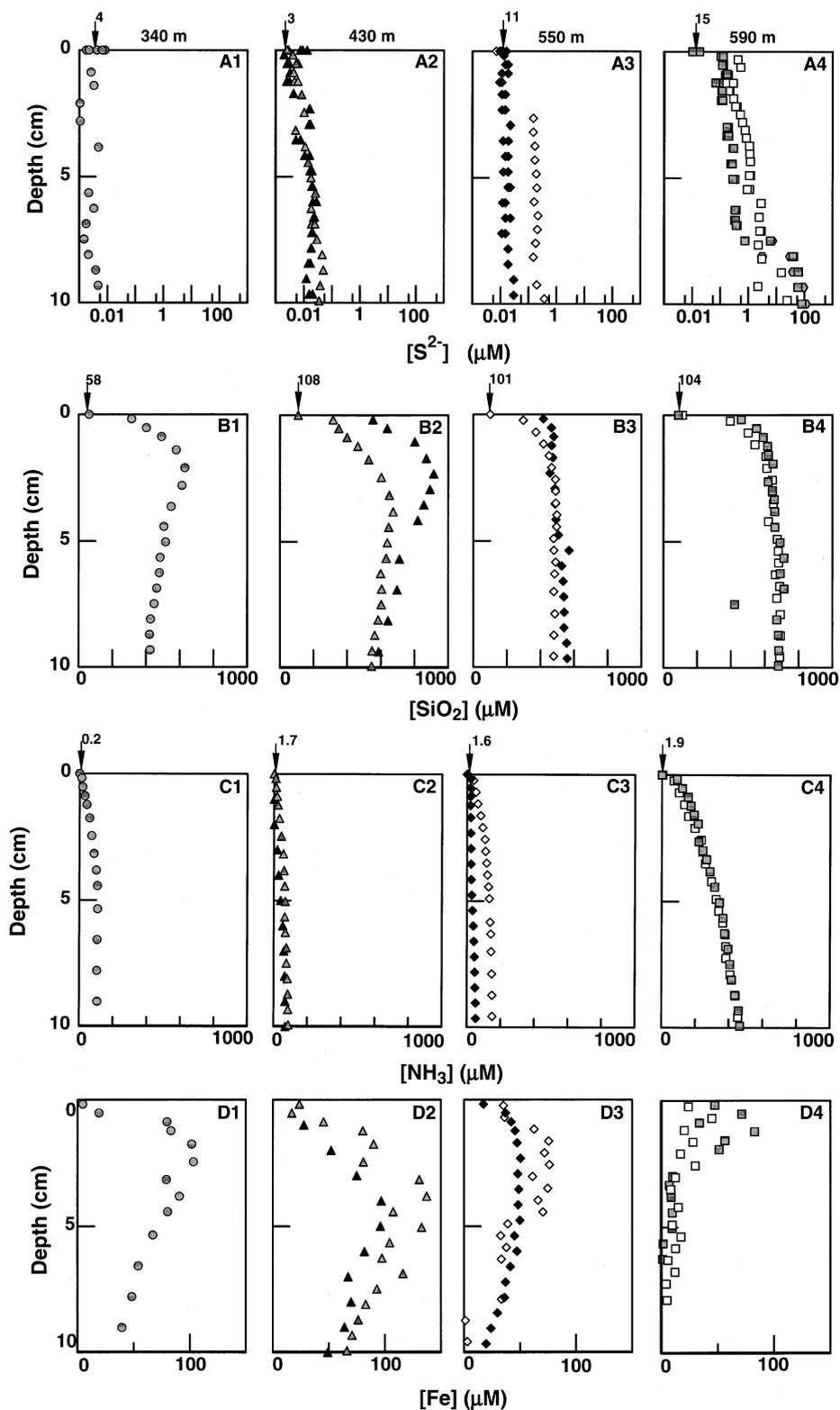
Fig. 3. Pore-water profiles in the Santa Barbara Basin for dissolved sulfides (note log scale, panel A), silicate (panel B), ammonia (panel C), and iron (panel D) from cores taken at various basin depths. Using symbols consistent with Fig. 1, the panel columns 1, 2, 3, and 4 denote coring site depths 340 m (circle), 430 m (triangle), 550 m (diamond), and 590 m (square), respectively. Consistent with previous figures, open, shaded, and dark symbols denote data from February 1995, December 1995, and April 1997 sampling cruises, respectively. In plate A4, comparative colorimetric sulfide data at elevated concentrations (>2 μM) are shown as hexagons. Arrows and adjacent numbers on the top border of each plot indicate mean bottom-water concentrations (μM, but nM for sulfides). Bottom-water Fe concentrations are not available.

Table 2. Water-column nitrate consumption and benthic flux of ammonia based on pore-water gradients. The diffusive constants (Chung, 1973; Berelson et al., 1982; Li and Gregory, 1974) for flux estimates and site designations as indicated in Table 3 were used. Water-column gradients were based on data within the basin (Fig. 2A2) from the sediment–water interface to the sill depth (590–480 m), while pore-water gradients were based on data from the top 5 cm. The number of data points (n) and coefficient of determination (r^2) for each nonlinear gradient determination are also tabulated.

Date	Core	n; r^2	Gradient (μM cm^{-1})	Flux (μmole m^{-2} h^{-1})
Water-column nitrate gradients (590 m site)				
2/16/95		8; 0.62	-1.05×10^{-3}	-140
11/30/95		10; 0.87	-0.57×10^{-3}	-80
4/26/97		4; 0.99	-0.47×10^{-3}	-60
Pore-water ammonia gradients				
2/16/95	B590-1	12; 0.99	122	44
2/17/95	B550-1	13; 0.98	69	25
12/1/95	M590-2	14; 0.96	198	71
11/30/95	M430-2	12; 0.99	21	7
12/2/95	M340-2	12; 1.00	40	14
4/27/97	M550-3	14; 0.95	282	102
4/26/97	M430-3	10; 0.99	57	20

(1973) and Berelson et al. (1982) reported similar determinations for K_z for the Santa Barbara Basin based on radon-222 studies (3.9 and 3.4 cm^2 s^{-1}, respectively). Using an average of those determinations (3.7 cm^2 s^{-1}), the sulfide flux ranges from 100 to 300 nmole m^{-2} h^{-1} (Table 3). These estimates, based on water-column gradients, may represent an upper limit of sulfide flux if that sulfide within the suboxic, deep-basin water column oxidizes at a rate faster than water-column sulfate reduction occurs (Hastings and Emerson, 1988). This is because such net sulfide oxidation in the water column would tend to steepen the water-column sulfide gradients, thereby increasing our flux estimates. However based on evidence described in the following paragraph, it is our contention that these flux determinations are reasonable.

Kinetics of water-column sulfide oxidation are dependent on a number of environmental parameters (e.g., DO concentration, pH, temperature, sulfide speciation, and the presence of microbial mats, Fe(III)–oxyhydroxide and Mn–oxide phases). Oxidation of hydrogen sulfide in oxidized seawater (DO > 200 μM, $\geq 25°$C) has been shown in laboratory experiments to occur over time scales of hours to days (Zhang and Millero, 1993). Yet, sulfide in near-surface seawater can persist at low (i.e., submicromolar) concentrations for months, even in the presence of O_2, H_2O_2, and IO_3^-, probably due to the presence of kinetically stable metal–sulfide complexes (Dyrssen, 1988; Luther and Tsamakis, 1989; Luther et al., 1996). Below sill depth, sulfide oxidation is further retarded in the presence of decreased oxidant concentrations (Figs. 2A1 and 2A2), lower temperatures (6°C at the bottom and 12–16°C at the surface) and the absence of light to photolytically dissociate the metal–sulfides (Luther and Tsamakis, 1989). Vazquez et al. (1989) observed that when dissolved zinc was present at concentrations equivalent to dissolved sulfide, the overall rate constant (i.e., the first order rate constant divided by DO concentration) for sulfide oxidation in seawater was retarded by a factor of 30 relative to conditions without metal complexation effects. A half time of about 30 d for sulfide in surface waters was thereby estimated. Disregarding additional temperature and light inten-

Table 3. Sulfide flux for various locations within the Santa Barbara Basin based on water-column and pore-water gradients. For water-column estimates, a vertical eddy diffusivity of 3.7 cm^2 s^{-1} was used (Chung, 1973; Berelson et al., 1982) with the concentration gradient from the sediment–water interface to the sill depth (590–480 m) determined by exponential fit (Klump and Martens, 1981). For pore-water estimates, a diffusion coefficient of 1×10^{-5} cm^2 s^{-1} (Li and Gregory, 1974) was used with the pore-water gradient determined from an exponential fit of data near the sediment–water interface (<1 cm depth). Estimates for October 1988 are from representative pore-water profiles (upper 5 cm due to micromolar colorimetric detection limits for sulfides) from replicate cores by Reimers et al. (1990) taken near our 590 m site. The number of data points (n) and coefficient of determination (r^2) for each nonlinear gradient determination are also tabulated.

Date	Core	n; r^2	Gradient (μM cm^{-1})	Flux (μmole m^{-2} h^{-1})
Water-column gradients (590 m site)				
2/16/95		9; 0.90	2.2×10^{-6}	300
11/30/95		16; 0.25	2.3×10^{-6}	300
4/26/97		13; 0.81	1.0×10^{-6}	100
Pore-water gradients				
10/88A	—	10; 0.89	36	13000
10/88B	—	10; 0.59	16	6000
2/16/95	B590-1	3; 1.00	2.36	900
2/17/95	B550-1	3; 1.00	0.49	200
12/1/95	M580-2	9; 0.93	1.54	600
11/30/95	M430-2	8; 0.83	6×10^{-3}	2
12/2/95	M340-2	9; 0.10	-0.01	-4
4/27/97	M550-3	8; 0.01	0.01	4
4/26/97	M430-3	9; 0.08	9×10^{-3}	3

sity differences, if their experimental conditions (25 μM total dissolved sulfides and 212 μM DO) are related to Santa Barbara Basin bottom-water conditions ($\sim 10^{-2}$ μM total dissolved sulfides and <10 μM DO), the first order model would indicate an increase in the reaction half time to approximately 1.7 yr and oxidation rates four orders of magnitude slower than observed in laboratory experiments by Vazquez et al. With a mean water residence time of 0.8–6 yr in the bottom 100 m of the Basin (van Geen et al., 1995), this finding is consistent with that of Theberge et al. (1997), indicating that inert Zn and Cu sulfides in seawater allow dissolved sulfides to persist in the presence of oxygen.

Another way to estimate the flux of sulfide added to the water column is to use pore-water profiles for diffusion-gradient calculations. Given the surficial (<1 cm depth) porosity ranges from 0.87 to 0.96 for all coring sites (Zheng, in preparation, 1998) a sediment-diffusion coefficient of 1×10^{-5} cm^2 s^{-1} was used (Li and Gregory, 1974). The pore-water concentration gradient was computed by an exponential fit of the concentration data (Klump and Martens, 1981) near the sediment–water interface (i.e., <1 cm depth) and an assumed porosity of 1. Benthic flux studies over similar porosity ranges at Cape Lookout Bight (Klump and Martens, 1989) indicated that depth dependence of porosity did not have a significant effect on sulfate-reduction rate parameters relative to a constant mean-porosity assumption. The only exception to this interfacial-depth range was for B550-1, where lack of data between 0.3 and 2.1 cm required a <3.2 cm sediment depth range to be used for the exponential fit. This near-interface gradient was selected to avoid profile discontinuities (Fig. 3A4) and to examine surficial zones above observed peaks in dissolved Fe (Fig. 3D). Sulfide flux estimates for our study range from <10 nmole m^{-2} h^{-1} at the 340 and 430 m sites to 900 nmole m^{-2} h^{-1} at the deepest site. Even though the areal extent of the basin below 550 m is only about 6% of the basin total projected area, these orders-of-magnitude differences in flux estimates (Table 3) show that the deep basin is the dominant source of sulfide to the water column.

There is a striking similarity between the water-column profiles for dissolved sulfides (Fig. 2A3) and water-column enrichment of total particulate Fe within the Santa Barbara Basin (Shiller et al., 1985). Regeneration of dissolved iron from the basin sediments has been hypothesized as the Fe source by Shiller et al. (1985), but this explanation was complicated by the fact that there was no correspondence between particulate Fe and particulate S in the suspended material. They explained this lack of correspondence by another hypothesis that "basin bottom waters contain enough oxygen to rapidly oxidize sulfides at the sediment–water interface." In the context of our results, an alternative explanation is offered for the apparent deficiency in particulate S relative to Fe. In both seawater and freshwater, Fe forms labile bisulfide and sulfide complexes, unlike inert sulfide complexes with Cu and Zn (Davison, 1991; Luther et al., 1996; Theberge et al., 1997). When these labile Fe complexes dissociate in the presence of oxygen near the sediment–water interface, the sulfide product may then: (1) serve as an electron donor for surficial microbial mats as discussed below, or (2) form more inert metal–sulfide complexes that are transported and persist in the water column (Luther et al.,

1996). The sedimentary source of Fe (Fig. 3D) and particulate S to the bottom water is thereby decoupled.

Increased water-column dissolved-sulfide concentrations below sill depth were coincident with decreased nitrate concentrations (Figs. 2A2 and 2B2), providing further evidence for reactions and products that would otherwise be constrained to anaerobic environments. A water-column approach, analogous to the sulfide-flux determinations above, was used to estimate net nitrate consumption in the basin below the sill (Table 2). For consistency with sulfide flux determinations, the nitrate water-column gradient was evaluated at the sediment–water interface. The range of values determined from this study (-60–-140 μmole m^{-2} h^{-1}) is within the range of measured denitrification rates for coastal marine sediments (Seitzinger, 1988; 0–1,000 μmole m^{-2} h^{-1}). In nearby Santa Monica Basin, Jahnke (1990) measured a similar nitrate benthic flux of 46 ± 13 μmole m^{-2} h^{-1}. In earlier studies using a linear model for the concentration gradient and a K_z of 3 cm^2 s^{-1}, Liu (1979) calculated higher denitrification rates in the water column of the Santa Barbara Basin (-228 and -514 μmole m^{-2} h^{-1}). However, the benthic flux of ammonia (Table 2) and subsequent microbial nitrification could augment water-column nitrate.

Consistent with trends in sulfide pore-water concentrations, ammonia concentrations in the pore waters were greater at the 590 m site than at other sites (Fig. 3C). The concentration differences between sites result in different estimates of the benthic flux of ammonia (Table 2), with the exception of the calculated ammonia flux for M550-3. Although the maximum ammonia concentration for M550-3 (53.3 μM) in the top 10 cm was an order of magnitude less than observed at the 590 m site, the exponential fit for gradient determination emphasizes the concentration increase (20 μM) between the overlying water concentration and the first pore-water increment at 0.176 cm. This bias is demonstrated by the fact that the ammonia flux estimate by exponential fit for M550-3 (102 μmole m^{-2} h^{-1}) was two orders of magnitude greater than by linear fit (2 μmole m^{-2} h^{-1}). Profiles at shallower sites also provide an indication of ammonia generation in the sediments, but to a much lesser degree than at the 590 m site (Fig. 3C). Similar ammonia profiles, attributed to microbial degradation of benthic organic material, have been observed in previous studies near our deepest sampling site (Reimers et al., 1996), as well as in other suboxic environments like Cape Lookout Bight (Klump and Martens, 1981) and Saanich Inlet (Murray et al., 1978).

Formation of metal–sulfide precipitates has been proposed as a mechanism by which the benthic flux of dissolved sulfide is restricted from sediments within suboxic enviroments (Goldhaber and Kaplan, 1975; Berner, 1984; Thamdrup et al., 1994a; Reimers et al., 1996). Thamdrup et al. (1994a) observed sequential peaks in pore-water Mn^{2+}, Fe^{2+}, and dissolved sulfides with increasing depth in cores from Aarhus Bay, Denmark, and attributed them to microbially mediated processes occurring along the vertical redox gradient. With a similar vertical sequencing for dissolved pore-water Fe and total sulfide at other suboxic sites (Canfield, 1989), the prevailing hypothesis is that hydrogen sulfide accumulates in pore waters as reactive iron becomes depleted at depth, and pyrite formation ceases. Consistent with those observations, sulfide concentrations >1 μM in cores B590-1 and M580-2 were observed

about 6 cm below dissolved Fe maxima (Figs. 3A and 3D). The magnitude of this sulfide "trap" due to formation of iron–sulfide precipitates at the 590 m site can be estimated by the consumption rate or downward flux of dissolved Fe (Fig. 3D). An exponential model (Klump and Martens, 1981) was used to determine the concentration gradient from the depth of maximum pore-water dissolved Fe down to a 10 cm depth. The removal of sulfide by this mechanism ranges from 29 to 36 μmole m^{-2} h^{-1} (M580-2 and B590-1, respectively), clearly indicating the importance of this geochemical process in reducing the upward flux of dissolved sulfides to the sediment–water interface. The benthic sulfide flux that escapes trapping as precipitated Fe–sulfide for M580-2 and B590-1 (0.6–0.9 μmole m^{-2} h^{-1}, Table 3) determined from the gradients in the 0–1 cm interval, is two orders of magnitude smaller than the upward flux of sulfide to the Fe–sulfide trap.

At the shallow 430 and 340 m sites, steep concentration gradients in pore waters for dissolved sulfides >1 μM were not observed. Using the same flux calculation method as described in the previous paragraph, the presence of a dissolved Fe gradient below the pore-water maximum at the 430 and 340 m sites (Fig. 3D) corresponds to a sulfide consumption rate of 4.6, 4.7, and 5.1 μmole m^{-2} h^{-1} for cores M430-2, M340-2, and M430-3, respectively. The lack of a corresponding positive sulfide gradient below the dissolved Fe maximum (Fig. 3A, Table 3) suggests that sulfate reduction rates are much slower at these bioturbated sites relative to the deep basin. An estimate for the difference in sulfate reduction rates between shallow and deep basin sites can be determined by comparing the sum of rates for net sulfide production and dissolved Fe consumption (absolute value) at each site. There was minimal net sulfide production at the shallow sites relative to Fe consumption (Figs. 3A and 3D). Consequently, the sum of those rates for sulfide production and Fe consumption are 36.3 and 31.8 μmole m^{-2} h^{-1} for B590-1 and M580-2, but $\leq$5.1 μmole m^{-2} h^{-1} for all cores from shallower sites. Differences in sulfide profiles between sites suggests that sulfate reduction rates at 550, 430, and 340 m are approximately 30 μmole m^{-2} h^{-1} less than the value at 590 m. By comparison, Reimers et al. (1996) reported sulfate reduction rates of 3–9 mM yr^{-1} in the top 10 cm of a core collected near the 590 m site in June 1988. The depth integration of these rates (0–10 cm) represents sulfide generation of 54 μmole m^{-2} h^{-1}.

Considering the visual similarity of sediment characteristics as described by Thamdrup et al. (1994a) for Aarhus Bay with characteristics described herein for the shallow sites in the Santa Barbara Basin, it is notable that we did not observe significant sulfide gradients at the brown–grey color transition in cores from the 340 and 430 m sites as was observed in Aarhus Bay cores. Such elevated concentrations were only observed at the 590 m site. Furthermore, bottom-water DO concentrations were consistently lower in the Santa Barbara Basin (<30 μM) than in Aarhus Bay (>50 μM). Although dissolved sulfides within the top 10 cm were consistently detectable in pore waters of the Santa Barbara Basin, we may infer from this contrast that sulfate-reduction rates at our shallow sites did not exceed scavenging by metal–sulfide precipitation to the extent observed in Aarhus Bay. This site-specific contrast may have been due to lower bottom-water temperatures in the Santa Barbara Basin (5.7–6.4°C) than in Aarhus

Bay (5–15°C), lower biological availability of benthic organic carbon, or enhanced bioturbation at the shallow sites in the Santa Barbara Basin relative to Aarhus Bay.

Decreases in pore-water silicate concentrations below about 2–3 cm in M430-2, M340-2, and M430-3 (Fig. 3B) are a clear indication of irrigation. The more gradual core-top silicate gradients in the pore water at these sites, compared with the core-top Si gradients from B590-1, M580-2, and M590-3, may also reflect the importance of nondiffusive transport (irrigation) just below the sediment–water interface at the 340 and 430 m sites. This interpretation is consistent with contrasts in core characteristics reported herein between cores taken from shallow (340 and 430 m) versus deep-basin sites (550 and 590 m). Low bottom-water DO concentrations at 550 and 590 m sites relative to shallower sites (Fig. 2A1) restrict the abundance of benthic invertebrates that irrigate and bioturbate the sediments (Bernhard et al., 1997). The low irrigation rates associated with the low-oxygen deep basin sites results in higher pore-water sulfide concentrations and higher diffusive fluxes of sulfide into the overlying bottom water (Fig. 3A; Tables 2 and 3). Our benthic flux estimates are lower limits, particularly at the shallower sites, since we have not attempted to quantify nondiffusive transport.

4.2. Temporal Variability of Pore-Water Sulfides in the Deep Basin

Profiles for dissolved sulfides were previously published for the Santa Barbara Basin near our deepest site (590 m) on four cruises between February 1988 and June 1991 (Reimers et al., 1990; Reimers et al., 1996). Those pore-water profiles were similar in that colorimetrically detectable sulfide concentrations were typically observed within the sediments at depths less than 5 cm, and increased with depth to ~100–600 μM over the top 10 cm. Data from two of these cores (replicates taken near the deep basin site in October, 1988) also provide a sense of the small-scale (i.e., within-site) spatial variability relative to temporal variability of deep-basin redox conditions (Fig. 4). In contrast to Reimers' pore-water profiles for sulfide, the B590-1 and M580-2 profiles from February and December 1995 show lower concentrations below the sediment–water interface with concentrations approaching 1 μM at about 7–8 cm, and the maximum sulfide concentration in the top 10 cm of the two 1995 cores was 110.2 μM.

Temporal differences in pore-water sulfide profiles observed between sampling dates probably cannot be attributed to small-scale spatial variability of redox conditions. In proximity to our 590 m site, Reimers et al. (1996) observed seasonal shifts in pore-water chemistry in response to variability in bottom-water chemistry. Pore-water sulfide gradients from two replicate cores taken by Reimers et al. (1990) show just a factor of 2 variation (Table 3). In studies of Aarhus Bay, Thamdrup et al. (1994b) observed greater variability in laboratory determinations of the Mn^{2+} benthic flux (0.20–0.60 mmol m^2 d^{-1}) relative to either in situ chamber estimates (0.33–0.42 mmol m^2 d^{-1}) or the diffusive flux measurements based on pore-water profiles (1.0–1.2 mmol m^2 d^{-1}). Variability in laboratory estimates was explained by the "patchiness" of organic matter distribution and infaunal activity that was inadequately integrated by the sediment core with a 23 cm^2 internal cross-
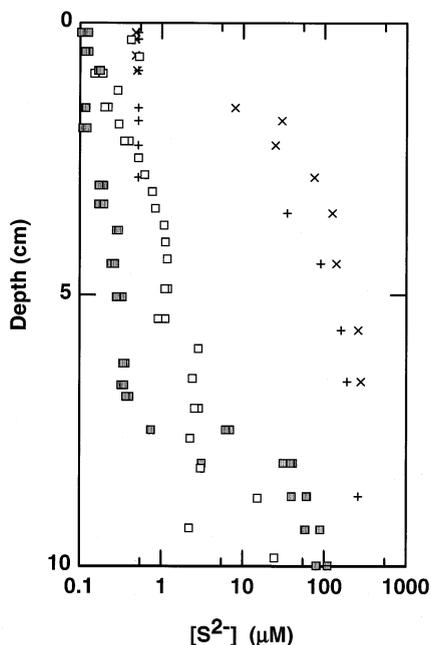
Fig. 4. Variability in pore-water sulfide gradients near the sediment–water interface at 590 m are shown with profiles from two replicate cores taken in October, 1998 by Reimers et al. (1990) shown with cross and "x" markers. Open and shaded squares represent data from February 1995 and December 1995 sampling cruises, respectively. The mean bottom-water concentration from three sampling cruises at this site was approximately 15 nM (Fig. 3A4).

sectional area. Even if one assumes similar small-scale spatial variability in profiles (20% to threefold) from the Santa Barbara Basin cores with a greater internal cross-sectional area (71 cm^2), the order of magnitude differences in the sulfide profiles observed at the 590 m site during various sampling trips cannot be attributed solely to "patchiness" (Fig. 4, Table 3).

The sulfide benthic flux calculated from pore-water gradients near the sediment–water interface (<1 cm) for B590-1 and M580-2, were 900 and 600 nmole m^{-2} h^{-1}, respectively, but ≥6,000 nmole m^{-2} h^{-1} for both 1988 cores (Reimers et al., 1990; Table 3). This disparity suggests that the deep basin was characterized by more reducing conditions in 1988 relative to 1995. Similarly, the sulfide flux estimates, based on below-sill water-column gradients (100–300 nmole m^{-2} h^{-1}), were also consistently an order of magnitude lower than indicated by the 1988 pore-water data. In fact, if higher-resolution, near-interface sulfide concentrations were available for the 1988 cores, the exponential model would yield an even greater disparity due to increasing slope near the interface. This disparity between the water-column flux estimates reported here and the pore-water flux estimates for October 1988 could simply be due to the lack of water-column sulfide data for 1988 (i.e., water-column sulfides may have been much higher in October 1988 than observed on any of our three sampling trips). However, the consistency of the water-column based flux estimates (10^2 nmole m^{-2} h^{-1}), even in April 1997, when the most reducing conditions were observed, suggests that sulfide oxidation occurs below sill depth when steep sulfide gradients are established in the deep-basin sediment. This explanation is supported by observations that elevated pore-water sulfide concentrations and low bottom-water DO were coincident with increased populations of *Beggiatoa* that are known to use sulfide as an electron donor (Jørgensen and Revsbech, 1983; Nelson and Jannasch, 1983; Møller et al., 1985). These populations of sulfide oxidizers may serve as a biological barrier to the sulfide flux.

Calculation of the sulfide fluxes were based on the depth interval between 0 and 1 cm to focus on concentration gradients near the surficial microbial mat, and shallower than the concentration peaks for dissolved Fe (Fig. 3D4). These peaks, which indicate Fe reduction with deeper formation of Fe sulfides, represent an important mechanism by which the source of sulfide to the sediment–water interface may be reduced in magnitude below the dissolved Fe peaks (Sec. 4.1 above; Reimers et al., 1996). Above this iron–sulfide trap, additional evidence of the importance of the benthic microbial layer is gleaned from the observation that all three sulfide flux estimates based on water-column profiles are less than any of the sulfide fluxes determined from pore-water gradients (<1 cm sediment depth) in this study, or by Reimers et al. (1990) at the 590 m site (Table 3). Given that sulfate reduction may occur in "microzones" when dissolved oxygen is present in the bulk solution (Hastings and Emerson, 1988), one might expect the opposite result (i.e., higher water-column based fluxes). A sulfide uptake rate of 1.5×10^6 nmole m^{-2} h^{-1} was determined for a thin (0.05 cm) *Beggiatoa* mat in cores incubated at 20°C by Jørgensen and Revsbech (1983) with bottom-water hydrogen sulfide concentrations of about 30 μM. It is difficult to quantitatively extrapolate such a flux down to the conditions of the Santa Barbara Basin, but even a sulfide uptake rate four orders of magnitude smaller than reported by Jørgensen and Revsbech (1983), by a thicker (>0.1 cm), tufted *Beggiatoa* mat in the Santa Barbara Basin (i.e., more biomass for sulfide uptake) could account for the disparity between the pore-water and the water-column based sulfide fluxes (i.e., an oxidation rate of approximately 10^2 nmole m^{-2} h^{-1}; Table 3). Although the *Beggiatoa* tufts have been extensively observed in the deep basin >550 m, the difference between the pore-water and the water-column based sulfide flux estimates at the 590 m site could be at least partly explained by spatial variability in the deep basin. The range of sulfide flux determinations for the 550 m site (4–200 nmole m^{-2} h^{-1}; Table 3), suggest that the areally averaged benthic flux of sulfide in the deep basin could be lower than indicated by the 590 m data where the hydrocasts were taken.

Analogous to arguments presented above regarding spatial variability, temporal differences in the pore-water profiles for sulfide may be affected by a microbial-community response to changes in bottom-water chemistry and pore-water oxidant concentrations. Sulfate reduction rates have long been measured in suboxic marine environments (Jørgensen, 1977), and in the Santa Barbara Basin were consistently >2 mM yr^{-1} at sediment depth <10 cm near our 590 m site (Reimers et al., 1996). If one assumes that this rate approximates the net microbial sulfide production rate (Jørgensen, 1977), then it would take only several weeks to shift the shallow gradient observed in February and December 1995 to that reported for October 1988 (i.e., <10–>100 μM; Fig. 4). The structure of benthic communities in the Santa Barbara Basin has been

characterized by bottom-water redox conditions (Bernhard and Reimers, 1991; Bernhard et al., 1997). It is therefore reasonable to assume that when changes in bottom-water chemistry alter redox gradients at the sediment–water interface, the composition of the benthic community may shift. These transitions near the interface are expected to alter biologically mediated reaction rates and the resulting benthic fluxes of reactants and products.

5. CONCLUSION

A comparison with water-column profiles at a site outside the Santa Barbara Basin (a control site) consistently indicated more reducing conditions within the basin. Dissolved sulfide, iron, and macronutrient distributions in the sediments were indicative of diverse redox conditions between the four coring sites within the Santa Barbara Basin. A sulfide concentration range of 5 orders of magnitude in pore waters was observed. Depth profiles for pore-water silicate and ammonia as well as for water-column nitrate and sulfide were consistent with observed spatial and temporal variability in redox conditions within the basin. Although we agree with Reimers' et al. (1996) hypothesis for the deep basin that the formation of iron–sulfide precipitates regulate the source of dissolved sulfides to the sediment–water interface, our results and observations also suggest that microbially mediated sulfide oxidation near the sediment–water interface attenuates the benthic sulfide flux. In contrast to the deep basin, micromolar pore-water sulfide peaks were absent at the shallower sites below observed peaks for dissolved Fe and appear to reflect changes in bottom-water chemistry at these more oxidized sites as well as the magnitude of bioturbation.

REFERENCES

Behl R. J. and Kennett J. P. (1996) Brief interstadial events in the Santa Barbara Basin, NE Pacific, during the last 60 kyr. *Nature* **379,** 243–246.

Berelson W. M., Hammond D. E., and Fuller C. (1982) Radon-222 as a tracer for mixing in the water column and benthic exchange in the southern California borderland. *Earth Planet. Sci. Lett.* **61,** 41–54.

Berner R. A. (1984) Sedimentary pyrite formation: An update. *Geochim. Cosmochim. Acta* **48,** 605–615.

Bernhard J. M. and Reimers C. E. (1991) Benthic foraminiferal population fluctuations related to anoxia: Santa Barbara Basin. *Biogeochemistry* **15,** 127–149.

Bernhard J. M., Sen Gupta B. K., and Borne P. F. (1997) Benthic foraminiferal proxy to estimate dysoxic bottom-water oxygen concentrations: Santa Barbara Basin, U.S. Pacific continental margin. *J. Foram. Res.* **27,** 301–310.

Broenkow W. W. and Cline J. D. (1969) Colorimetric determination of dissolved oxygen at low concentrations. *Limnol. Oceanogr.* **14,** 450–454.

Canfield D. E. (1989) Reactive iron in marine sediments. *Geochim. Cosmochim. Acta* **53,** 619–632.

Chung Y. (1973) Excess radon in the Santa Barbara Basin. *Earth Planet. Sci. Lett.* **17,** 319–323.

Cline J. D. (1969) Spectrophotometric determination of hydrogen sulfide in natural waters. *Limnol. Oceanogr.* **14,** 454–458.

Crusius J., Calvert S., Pedersen T., and Sage D. (1996) Rhenium and molybdenum enrichments in sediments as indicators of oxic, suboxic and sulfidic conditions of deposition. *Earth Planet. Sci. Lett.* **145,** 65–78.

Davison W. (1991) The solubility of iron sulphides in synthetic and natural waters at ambient temperature. *Aquat. Sci.* **53,** 309–329.

Dyrssen D. (1988) Sulfide complexation in surface seawater. *Mar. Chem.* **24,** 143–153.

Emerson S. R. and Huested S. S. (1991) Ocean anoxic and the concentrations of molybdenum and vanadium in seawater. *Mar. Chem.* **34,** 177–196.

Fofonoff N. P. and Millard R. C. Jr. (1983) Algorithms for computation of fundamental properties of seawater. *UNESCO Technical Papers in Marine Science*, No. 44, pp. 15–23. UNESCO.

Goldhaber M. B. and Kaplan I. R. (1975) Controls and consequences of sulfate reduction rates in recent marine sediments. *Soil Sci.* **119,** 42–55.

Hastings, D. and Emerson, S. (1988) Sulfate reduction in the presence of low oxygen levels in the water column of the Cariaco Trench. *Limnol. Oceanogr.* **33,** 391–396.

Helz G. R., Miller C. V., Charnock J. M., Mosselmans J. F. W., Pattrick R. A. D., Garner C. D., and Vaughan D. J. (1996) Mechanism of molybdenum removal from the sea and its concentration in black shales: EXAFS evidence. *Geochim. Cosmochim. Acta* **60,** 3631–3642.

Jacobs L., Emerson S., and Skei J. (1985) Partitioning and transport of metals across the O_2/H_2S interface in a permanently anoxic basin, Framvaren Fjord, Norway. *Geochim. Cosmochim. Acta* **49,** 1433–1444.

Jahnke R. A. (1990) Early diagenesis and recycling of biogenic debris at the seafloor, Santa Monica Basin, California. *J. Mar. Res.* **48,** 413–436.

Johnson K. S. and Petty R. L. (1983) Determination of nitrate and nitrite in seawater by flow injection analysis. *Limnol. Oceanogr.* **28,** 1260–1266.

Jørgensen B. B. (1977) The sulfur cycle of a coastal marine sediment (Limfjorden, Denmark). *Limnol. Oceanogr.* **22,** 814–832.

Jørgensen B. B. and Revsbech N. P. (1983) Colorless sulfur bacteria, *Beggiatoa* spp., and *Thiovulum* spp., in O_2 and H_2S microgradients. *Appl. Environ. Microbiol.* **45,** 1261–1270.

Karl D. M. (1978) Distribution, abundance, and metabolic states of microorganisms in the water column and sediments of the Black Sea. *Limnol. Oceanogr.* **23,** 936–949.

Kester D. R. (1975) Dissolved gases other than CO_2. In *Chemical Oceanography* (ed. J. P. Riley and G. Skirrow), 2d ed., Vol. 1, pp. 497–589, Academic.

Klump J. V. and Martens C. S. (1981) Biogeochemical cycling in an organic rich coastal marine basin—II. Nutrient sediment-water exchange processes. *Geochim. Cosmochim. Acta* **45,** 101–121.

Klump J. V. and Martens C. S. (1989) The seasonality of nutrient regeneration in an organic-rich coastal sediment: Kinetic modeling of changing pore-water nutrient and sulfate distributions. *Limnol. Oceanogr.* **34,** 559–577.

Kuwabara J. S. and Luther G. W. (1993) Dissolved sulfides in the oxic water column of San Francisco Bay, California. *Estuaries* **16,** 567–573.

Li Y. H. and Gregory S. (1974) Diffusion of ions in sea water and in deep-sea sediments. *Geochim. Cosmochim. Acta* **38,** 703–714.

Liu K. K. (1979) Geochemistry of inorganic nitrogen compounds in two marine environments: The Santa Barbara Basin and the Ocean off Peru. Ph.D. dissertation, Univ. Calif. Los Angeles.

Luther G. W., Giblin A. E., and Barsolona R. (1985) Polarographic analysis of sulfur species in marine porewaters. *Limnol. Oceanogr.* **30,** 727–736.

Luther G. W. and Tsamakis E. (1989) Concentrations and form of dissolved sulfide in the oxic water column of the ocean. *Mar. Chem.* **27,** 165–177.

Luther G. W., Church T. M., and Powell D. (1991) Sulfur speciation and sulfide oxidation in the water column of the Black Sea. *Deep-Sea Res.* **38,** S1121–S1137.

Luther G. W., Rickard D. T., Theberge S., and Olroyd A. (1996) Determination of metal (bi)sulfide stability constants of Mn^{2+}, Fe^{2+}, Co^{2+}, Ni^{2+}, Cu^{2+}, and Zn^{2+} by voltammetric methods. *Environ. Sci. Technol.* **30,** 671–679.

Millero F. J. (1991) The oxidation of H_2S in Black Sea waters. *Deep-Sea Res.* **38,** S1139–S1150.

Møller M. M., Nielsen L. P., and Jørgensen B. B. (1985) Oxygen responses and mat formation by *Beggiatoa* spp. *Appl. Environ. Microbiol.* **50,** 373–382.

Murray J. W., Grundmanis V., and Smethie W. M., Jr. (1978) Interstitial water chemistry in the sediments of Saanich Inlet. *Geochim. Cosmochim. Acta* **42,** 1011–1026.

Nelson D. C. and Jannasch, H. W. (1983) Chemoautotrophic growth of a marine *Beggiatoa* in sulfide-gradient cultures. *Arch. Microbiol.* **136,** 262–269.

Petersen L. C., Overpeck J. T., Kipp N. G., and Imbrie J. (1991) A high-resolution Late Quaternary upwelling record from the anoxic Cariaco Basin, Venezuela. *Paleoceanography* **6,** 99–119.

Piper D. Z. and Isaacs C. M. (1996) Instability of bottom-water redox conditions during accumulation of Quaternary sediment in the Japan Sea. *Paleoceanography* **11,** 171–190.

Reimers C. E., Lange C. B., Tabak M., and Bernhard J. M. (1990) Seasonal spillover and varve formation in the Santa Barbara Basin, California. *Limnol. Oceanogr.* **35,** 1577–1585.

Reimers C. E., Ruttenberg K. C., Canfield D. E., Christiansen M. B., and Martin J. B. (1996) Porewater pH and authigenic phases formed in the uppermost sediments of the Santa Barbara Basin. *Geochim. Cosmochim. Acta* **60,** 4037–4057.

Richards F. A. (1965) Anoxic Basins and Fjords. In *Chemical Oceanography* (eds. J. P. Riley and G. Skirrow), Vol. 1, pp. 611–645. Academic.

Rosenthal Y., Lam P., Boyle E. A., and Thomson J. (1995) Authigenic cadmium enrichments in suboxic sediments: Precipitation and post-depositional mobility. *Earth Planet. Sci. Lett.* **132,** 99–111.

Seitzinger S. P. (1988) Denitrification in freshwater and coastal marine ecosystems: Ecological and geochemical significance. *Limnol. Oceanogr.* **33,** 702–724.

Shiller A. M., Gieskes J. M., and Price N. B. (1985) Particulate iron and manganese in the Santa Barbara Basin, California. *Geochim. Cosmochim. Acta* **49,** 1239–1249.

Shimmield G. B. and Price N. B. (1986) The behavior of molybdenum and manganese during early sediment diagenesis—Offshore Baja California, Mexico. *Mar. Chem.* **19,** 261–280.

Sholkovitz E. R. and Gieskes J. M. (1971) A physical-chemical study of the flushing of the Santa Barbara Basin. *Limnol. Oceanogr.* **16,** 479–489.

Soutar A. (1971) Micropaleontology of anaerobic sediments and the California Current. In *The Micropaleontology of Oceans* (eds. B. M. Funnell and W. R. Ridell), pp. 223–230. Cambridge.

Strickland J. D. and Parsons T. R. (1968) *A Practical Handbook of Seawater Analysis*. Bull. Fish. Res. Bd. Can. 167.

Thamdrup B., Fossing H., and Jørgensen B. B. (1994a) Manganese, iron and sulfur cycling in a coastal marine sediment, Aarhus Bay, Denmark. *Geochim. Cosmochim. Acta* **58,** 5115–5129.

Thamdrup B., Glud R. N., and Hansen J. W. (1994b) Manganese oxidation and *in situ* manganese fluxes from a coastal sediment. *Geochim. Cosmochim. Acta* **58,** 2563–2570.

Theberge, S. M., Luther G. W., and Farrenfopf A. M. (1997) On the existence of free and metal complexed sulfide in the Arabian Sea and its oxygen minimum zone. *Deep-Sea Res.* **44,** 1381–1390.

Thunell R. C., Tappa E., and Anderson D. M. (1995) Sediment fluxes and varve formation in Santa Barbara Basin, offshore California. *Geology* **23,** 1083–1086.

van Geen A., McCorkle D. C., and Klinkhammer G. P. (1995) Sensitivity of the phosphate–cadmium–carbon isotope relation in the ocean to cadmium removal by suboxic sediments. *Paleoceanography* **10,** 159–169.

Vazquez F. G., Zhang J., and Millero F. J. (1989) Effect of metals on the rate of the oxidation of H_2S in seawater. *Geophys. Res. Lett.* **16,** 1363–1366.

Zhang J. Z. and Millero F. J. (1993) The products from the oxidation of H_2S in seawater. *Geochim. Cosmochim. Acta* **57,** 1705–1718.

Zheng Y., Anderson R. F., van Geen A., and Kuwabara J. S. (1999). Authigenic Mo formation in marine sediments: A link to pore-water sulfide in the Santa Barbara Basin. *Geochim. Cosmochim. Acta* (in preparation).